Parametric Study of Electro Discharge Boring of Inconel 718 with Radial Tool Movement Using Taguchi Method

Sudhanshu Kumar, Harshit K. Dave, and Keyur P. Desai

Abstract Electro discharge machining is an unconventional machining process in which material is removed by spark erosion. In the present research work, EDM process has been used for carrying out boring operation of Ni based superalloy (Inconel 718). Boring operation has been performed by guiding and controlling the movement of tool electrode on radial orbital tool path. Experiments have been conducted using Taguchi's method to obtain the influence of orbital and non-orbital parameters on material removal rate (MRR), tool wear rate (TWR) and surface roughness (Ra). ANOVA has been performed to identify the statistically significant parameters. It has been observed that all selected parameters are statistically significant in which peak current contributes 52.26% followed by flushing time i.e. 17.27% in determining the MRR. The peak current, pulse on time and orbital speed has been identified as significant parameters for TWR. The percentage contribution of peak current has been obtained maximum as 42.80% followed by pulse on time (38.48%) for TWR. The variation of surface roughness has been significantly affected by peak current, pulse on time, pulse off time and orbital speed. The peak current contributed about 80.21% followed by pulse on time about 15.03% for determining surface roughness. Estimation and confirmation experiments have been performed to verify the optimal combination of parameters.

S. Kumar (✉)
Department of Mechanical Engineering, M. A. National Institute of Technology, Bhopal, Madhya Pradesh 462003, India
e-mail: sudhanshuk27@gmail.com

H. K. Dave · K. P. Desai
Department of Mechanical Engineering, S. V. National Institute of Technology, Surat, Gujarat 395007, India
e-mail: harshitkumar@yahoo.com

K. P. Desai
e-mail: kpd@med.svnit.ac.in

253

1 Introduction

Electro-Discharge machining (EDM) process is one of the most widely used non-conventional machining process for machining of newly developed high strength alloys with high degree of dimensional accuracy. Machining of electrically conductive material irrespective of its hardness, by the application of thermal energy, is one of the prime advantages of this process [1]. Thus this process finds a suitable application in machining of Ni based superalloy i.e. Inconel 718 that is difficult to machine conventionally because of high hot hardness, high strength and poor thermal conductivity. Due to retention of hardness at higher temperature, Ni alloys are mostly used in aerospace vehicles [2].

Basically, in die-sinking EDM process, tool electrode has only vertical (jumping) movement. Therefore, it creates cavity that is mirror image of the shape of the tool electrode. However, if tool electrode is provided some orbital movement around its axis then a larger size of cavity is possible with smaller diameter of tool electrode. In orbital EDM, tool electrode continuously orbits while machining [3]. When the movement of tool electrode is controlled on circular path with continuously increasing in vertical axis (movement in X, Y, Z axis simultaneously) then this is termed as helical orbital EDM [4]. If tool electrode is allowed to move on circular path with continuously increasing radius (X, Y axis) then this machining is named as spiral orbital machining [5]. If the movement of tool electrode is controlled in such a way that it removes the material by slicing into cylinder with different radii, this cutting process is named as cylindrical orbital machining in EDM [6]. There is another possibility of tool path in orbital EDM i.e. radial tool path. In radial tool movement, tool electrode removes the material while actuating on the locus of radius of a circle. This movement of tool electrode can be applied for enlargement of a predrilled circular cavity that is boring operation. In the present investigation, boring of predrilled hole has been performed with radial tool movement in EDM process. Being EDM as a thermoelectric process [7], several electrical parameters are involved during machining such as peak current, pulse on time, pulse off time, gap voltage etc. If tool electrode is given some movement then some non-electrical parameters (orbital parameters) like orbital radius, orbital speed, flushing time etc. come into picture. Involvement of large number of parameters makes the EDM process more complex. Therefore it is important to identify the various factors influencing the response characteristics in order to understand the trend of process variable.

Literature indicates that several researchers have studied the influence of process parameters in EDM process. Belgassim and Abusaada [8] investigated the effect of electro discharge machining parameters on overcut for AISI D3 tool steel. Authors observed that overcut is significantly affected by peak current and pulse on time. Sing et al. [9] observed that the spark contact area of the tool electrode and workpiece plays critical role in material removal rate in EDM process. Effect of EDM parameters like peak current, pulse on time, pulse off time, gap voltage on performance measures like material removal rate, tool wear rate, surface roughness etc. in die-sinking EDM process is well explained in literature [10–13]. However, most of

the work is concentrated on die-sinking EDM process and little research works have been reported on orbital movement of tool electrode in EDM process. Rajurkar and Royo [14] used orbital tool movement with RF (Radio Frequency) control circuit in EDM process and observed improvement in surface integrity of machined surface. Yu et al. [15] used orbital tool movement for drilling of complex shape blind micro holes in EDM and observed that MRR increases and TWR decreases. Bamberg et al. [16] obtained an encouraging result with orbital tool movement in EDM process, due to improvement in dielectric flushing the material removal rate in micro hole drilling enhanced. The effect of other orbital parameter like orbital speed has not been discussed. Further, Bamberg and Heamawatanachai [6] investigated the orbital electrode actuation to improve efficiency of micro-holes varying orbital radius from 0 to 20 µm. It was reported that machining time and hole diameter has increased with the orbit radius. While radial overcut has decreased for higher orbital radius. The paper does not provide the details of orbital speed of tool electrode. El-Taweel et al. [5] conducted an investigation with spiral and helical modes of tool actuation in EDM process. It was reported that machining time has significantly reduced during orbital EDM. An incensement about 34% in MRR reported during the helical mode of tool actuation. Further, Dave et al. [4] performed the detailed study about the effect of electrical and orbital parameters on MRR and TWR using helical orbital strategy in EDM process. It was observed that orbital radius has significant effect on MRR but has insignificant effect in case of TWR .

The cutting ability and surface quality of machined surface of orbital tool movement over die sinking EDM process are reported. Most of the works are reported for drilling of circular holes with the help of EDM process. However, to the best of author's knowledge, published research on orbital tool movement in EDM process at radial path are very limited so far. The present work discusses the novel application of orbital tool movement at radial tool path in EDM process for boring operation of pre-drilled cavity, named as electro discharge boring. Therefore, in present study it is aimed to investigate the effect of process parameters during tool movement on radial path. Attempt is made to find parametric conditions for highest MRR with least TWR and surface roughness for electro discharge boring of existing hole.

2 Experimental Details

2.1 Experimental Setup

The experiments are performed on a Joemars, Taiwan make ZNC EDM machine, model JM 322, as shown in Fig. 1a. A special orbital head is attached to the quill of the EDM machine to provide orbit movement to the tool electrode as shown in Fig. 1b. Orbital unit consists of two stepped motors, each for guiding the tool electrode in X and Y direction during machining. Dial gauges are attached for monitoring the movement of the tool electrode; it indicates one revolution is equal to 1 mm tool
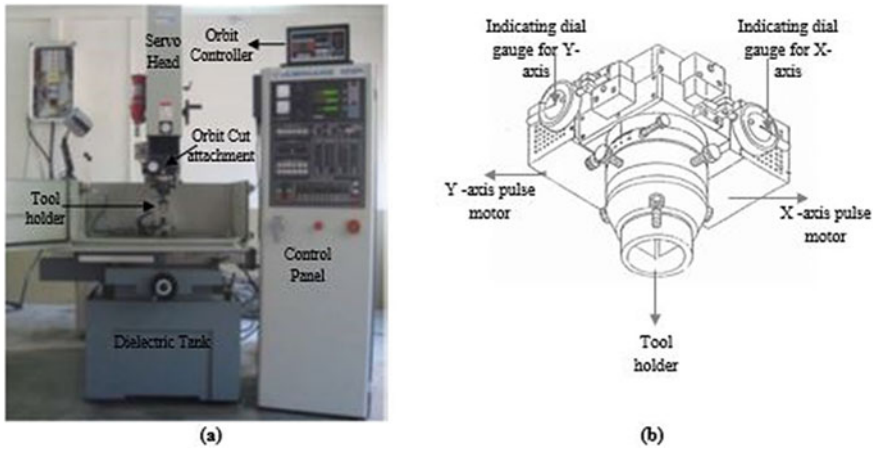
Fig. 1 Experimental set-up. **a** Electrical discharge machine. **b** Orbit cut attachment

travel. The movement of tool electrode as well as other necessary orbit parameters like radius, speed, flushing time, machining time etc. is controlled by an orbit cut controller. The maximum displacement of tool under orbiting condition is 4.999 mm from its centre. Thus, it can machine up-to the 9.999 mm diameter. The orbital cut controller can control X, Y and Z axis movement independently with 1 μm precision.

2.2 Concept of Radial Tool Movement

The tool movement under radial orbital strategy is confined to two dimensional planes only; its vertical (Z axis) movement is restricted. Tool electrode is guided to move on the locus of radius of a circular profile. In this strategy, material is removed by the side sparking on the tool electrode. First, tool electrode moves to the desired depth into the predrilled cavity on path 1 as depicted in Fig. 2a. After achieving required position in Z axis, its vertical movement is locked and is allowed to move on path 2. Tool electrode moves radially outward to the cavity wall where sparking occurs and erosion of work material takes place. Tool electrode returns back to its initial position at centre of cavity after cutting specified dimension of cut. The next movement of tool electrode is guided at 5° of angular increment from the previous tool path. In similar manner tool electrode moves on 72 paths, resulting into a circular cavity.

In radial tool movement, tool electrode advances towards the machining zone in fluctuating manner i.e. to and fro motion on straight line as illustrated in Fig. 3. The machining time decides the forward motion, depicted with F (0–1), F (2–3) in Fig. 3, of tool electrode and flushing time decides the backward motion, indicated with B (1–2), B (3–4) in Fig. 3, of tool electrode during radial tool movement in EDM.
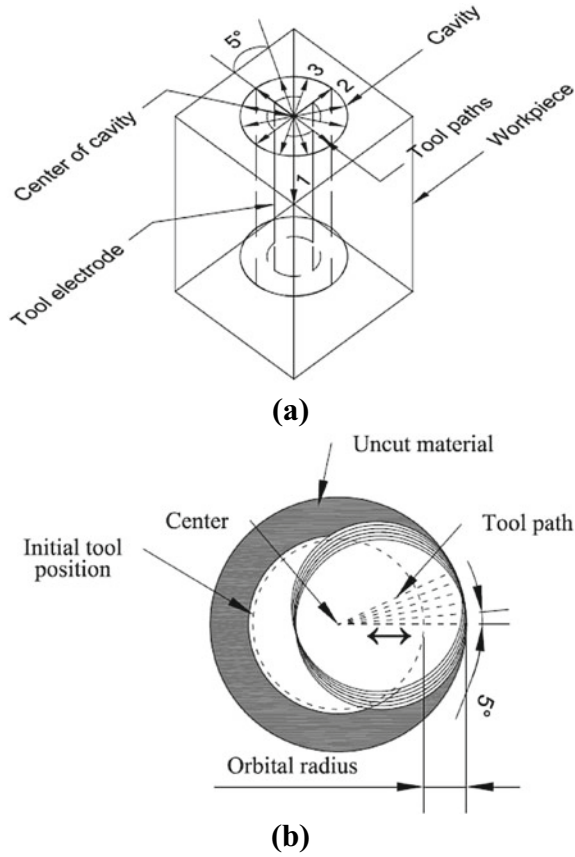
(a)

(b)

Fig. 2 Radial orbital strategy. **a** Isometric view. **b** Top view

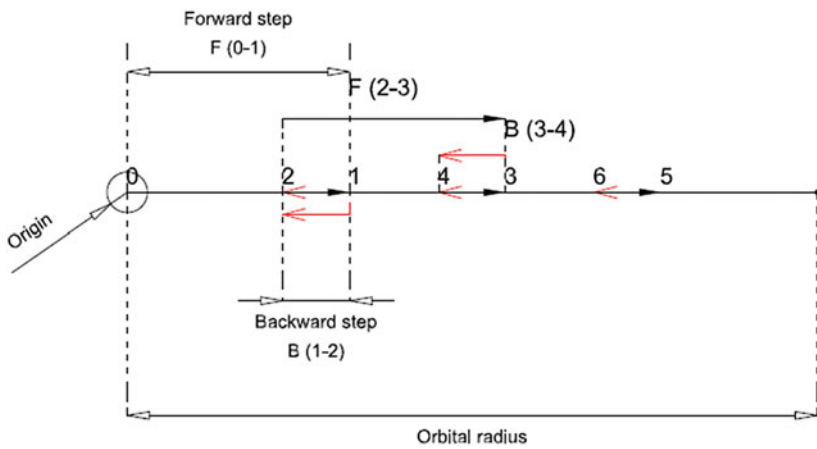**Fig. 3** To and Fro movement of tool electrode in radial orbital EDM

Table 1 Chemical composition of Inconel 718 (Wt.%)

Ni	Mo	Ti	C	Si	Cu	Cr	Co	Nb	Al	Mn	B
50–55	2.8–3.3	0.65–1.15	0.08	0.35	0.3	17–21	1	4.75–5.5	0.2–0.8	0.35	0.006

2.3 Tool and Workpiece

Inconel 718 and pure electrolytic copper (99.9% Cu) are used as workpiece material and tool material for the experiments. Inconel 718 is Ni based superalloy that exhibit excellent mechanical strength and creep resistance at high temperature. The chemical composition of Inconel 718 is shown in Table 1. Split workpiece has been used and initial cavity having 8.0 mm diameter is generated in a way that cavity is generated equally on both parts thereby providing a scope of studying the surface characteristics of cavity. A block of 10 mm × 15 mm × 15 mm dimension was cut from Inconel 718 bar using WEDM process. Each surface of block was highly polished and made parallel to respective side. Cylindrical tool electrode was fabricated into stepped shape having body and shank of 8 mm and 10 mm diameter respectively.

2.4 Experimental Procedure

Before experimentation, initial weight of workpiece and tool electrode is measured using digital weighing machine (having accuracy of 0.1 mg). Two blocks of workpiece are held on the machine table using clamping vice in such a way that edges of predrilled cavity match with each other. Tool electrode is fixed into the chuck attached with the EDM head. The workpiece and tool electrode are connected to negative and positive polarity respectively. Dielectric fluid is flushed through an external nozzle at machining zone. The depth of predrilled cavity is fixed to 10 mm. Machining duration is noted using stop watch. Figure 4 shows the tool positions in EDM set up for boring operation.
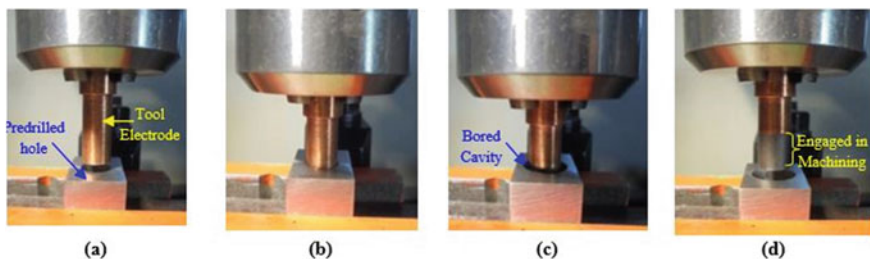

Fig. 4 Experimental procedure. **a** Predrilled cavity and tool electrode. **b** Tool electrode at full depth. **c** At the end of boring operation. **d** Bored cavity and tool wear

2.5 Input Parameters and Responses

EDM process uses spark energy to cut work metals therefore electrical parameters like peak current (I_p), pulse on time (t_{on}) and pulse off time (t_{off}) are considered for experimentations. Input parameters selected in present study with their range are listed in Table 2. Material Removal Rate (MRR), Tool Wear Rate (TWR) and Surface roughness (Ra) are selected as responses. MRR and TWR are expressed in mm3/min and calculated using following formula:

$$MRR = \frac{Initial\ weight\ of\ workpiece - Final\ weight\ of\ workpiece}{Machining\ time \times Density\ of\ Inconel\ 718} \quad (1)$$

$$TWR = \frac{Initial\ weight\ of\ tool\ electrode - Final\ weight\ of\ tool\ electrode}{Machining\ time \times Density\ of\ Copper} \quad (2)$$

Table 2 Input parameters and their values

S. no	Parameters	Values	Justification
1	A: Peak current (I_p)	6, 13, 21 A	Higher I_p values are omitted as they result into high tool wear and poor surface finish
2	B: Pulse on time (t_{on})	75, 195, 315 µs	Longer t_{on} improves the *MRR* but extra long t_{on} reduces the performance. Three levels of t_{on} are selected in lower to higher range available with the set up
3	C: Pulse off time (t_{off})	32, 82, 135 µs	t_{off} are selected in such a way that it should not be too short and too high
4	D: Orbital speed (S_o)	0.05, 0.09, 0.13 mm/s	Based on the similar study [4], S_o are selected from lower to higher values
5	E: Orbital radius (S_r)	0.50, 1.00, 1.50 mm	Higher setting of S_r increases tool travel time and reduces the *MRR*, therefore here S_r is varied from 0.50 to 1.50 mm
6	F: Machining time (t_m)	0.667, 1.034, 1.401 s	t_m should be sufficient to remove material. It is selected based on the tool movement capacity in existing set up to cover full available range
7	G: Flushing time (t_f)	0.067, 0.267, 0.467 s	Adequate flushing time is needed for effective and stable machining, higher t_f increases the total time that affects the *MRR*. Here, t_f is selected to cover full available range

Surface roughness of the machined cavities, expressed in micron, is measured in terms of arithmetic mean (Ra) using Mitutoyo surftest SJ 400 using a 90° diamond conical stylus with 5 μm tip radius. All the roughness measurements are carried out with the measuring length of 4 mm. The roughness parameter Ra is defined according to ISO 4287:1997 standard. Ra value is measured at six different locations (60° from each location) on the wall of cavity and average of all six values is taken as the surface roughness of cavity.

Taguchi technique is one of the most suitable methods for experimental study that reduce the number of experiments required to identify the optimal combination of parameters. The following steps are involved in Taguchi method:

1. Identification of process parameters and responses to be evaluated.
2. Selection of Orthogonal array as per number of parameters and their levels.
3. Allocation of process parameters to the orthogonal array and conduction of the experiment accordingly.
4. Calculation of signal-to-noise ratio (S/N ratio) according to quality characteristics of respective responses.
5. Analysis of results and identification of optimal combination of process parameters.
6. Verification of optimal parameters by conducting confirmation tests.

Taguchi method uses a set of orthogonal array for number of different experimental situations. Orthogonal array (OA) is designed in such a way that each level of a factor comes to equal number of times with all levels of other factors. Selection of suitable orthogonal array (from Taguchi's standard orthogonal array) is based on the total number of degree of freedom of experiments. Number of degree of freedom associated with a factor is one less than its total number of levels. In present case the degree of freedom for seven factors at 3 levels is 14 and for overall mean, degree of freedom is 1. Therefore, total degree of freedom is 15. The selected orthogonal array must have equal to or more experimental runs than the total number of degree of freedom required to study the responses. Thus the orthogonal array suitable for the study of seven parameters at three levels is L27 [17, 18], which implies 27 number of experiments should be performed. The layout of the experimental design is shown in Table 3. Each experiment is replicated twice. In Taguchi method, the calculated responses are converted into a variance index called Signal to Noise ratio (S/N ratio). The higher S/N ratio is always desirable in an experiment irrespective to quality characteristics. Higher value of S/N ratio indicates the more desirable condition. S/N ratio is categorized into three characteristics viz. lower the better (LB), nominal the better (NB), or higher the better (HB). MRR is HB characteristics while TWR and Surface roughness are LB characteristics. These are calculated using following formulae.

$$\eta_{HB} = -10 \log_{10} \left(\frac{1}{n} \sum_{j=1}^{n} \frac{1}{y_{ij}^2} \right) \tag{3}$$

Table 3 Experimental design and S/N ratios of responses

Experimental design								Responses		
Exp.	A	B	C	D	E	F	G	S/N ratio		
No.	I_p	t_{on}	t_{off}	S_o	S_r	t_m	t_f	η_{MRR}	η_{TWR}	η_{Ra}
1	6	75	32	0.05	0.50	0.667	0.067	8.3455	43.9367	−14.372
2	6	75	32	0.05	1.00	1.034	0.267	6.6694	47.6747	−13.931
3	6	75	32	0.05	1.50	1.401	0.467	6.6113	38.9468	−14.1494
4	6	195	82	0.09	0.50	0.667	0.067	11.9613	49.3940	−14.8742
5	6	195	82	0.09	1.00	1.034	0.267	11.1146	51.3478	−15.5642
6	6	195	82	0.09	1.50	1.401	0.467	10.6038	51.8306	−15.1476
7	6	315	135	0.13	0.50	0.667	0.067	12.4233	46.2204	−15.2207
8	6	315	135	0.13	1.00	1.034	0.267	12.0360	55.7311	−14.959
9	6	315	135	0.13	1.50	1.401	0.467	11.0092	60.0234	−14.5716
10	13	75	82	0.13	0.50	1.034	0.467	16.3828	12.2230	−16.4324
11	13	75	82	0.13	1.00	1.401	0.067	17.8716	12.9044	−17.3137
12	13	75	82	0.13	1.50	0.667	0.267	15.4827	14.3635	−16.8199
13	13	195	135	0.05	0.50	1.034	0.467	13.4423	50.5230	−18.2009
14	13	195	135	0.05	1.00	1.401	0.067	19.1462	34.9149	−19.5407
15	13	195	135	0.05	1.50	0.667	0.267	15.1009	36.7834	−18.6019
16	13	315	32	0.09	0.50	1.034	0.467	17.5429	46.9172	−19.6807
17	13	315	32	0.09	1.00	1.401	0.067	23.3368	41.2279	−19.3333
18	13	315	32	0.09	1.50	0.667	0.267	19.0122	60.5943	−18.6991
19	21	75	135	0.09	0.50	1.401	0.267	19.2708	0.0284	−18.0335
20	21	75	135	0.09	1.00	0.667	0.467	11.1047	8.4967	−17.9171
21	21	75	135	0.09	1.50	1.034	0.067	20.4063	8.1500	−18.1907
22	21	195	32	0.13	0.50	1.401	0.267	23.9444	11.9592	−20.6707
23	21	195	32	0.13	1.00	0.667	0.467	16.0962	25.0513	−20.0656
24	21	195	32	0.13	1.50	1.034	0.067	25.9092	16.7359	−20.8634
25	21	315	82	0.05	0.50	1.401	0.267	17.8311	33.8323	−21.1666
26	21	315	82	0.05	1.00	0.667	0.467	9.8914	50.0871	−21.5996
27	21	315	82	0.05	1.50	1.034	0.067	19.5090	34.2391	−20.9621

$$\eta_{LB} = -10 \log_{10} \left(\frac{1}{n} \sum_{j=1}^{n} y_{ij}^2 \right) \tag{4}$$

where, y_{ij} is the response of ith quality characteristics at jth experimental run and n is the total number of repetition of a run.

3 Results and Discussion

3.1 Analysis of Material Removal Rate (MRR)

To analyze the effect of input parameters main effect plots are plotted using average values of S/N ratio at each level and shown in Fig. 5. Analysis based on S/N ratio indicates that optimal conditions for higher MRR are peak current (I_p) 21A (Level 3), pulse on time (t_{on}) 195 μs (Level 2), pulse off time (t_{off}) 32 μs (Level 1), orbital speed (S_o) 0.13 mm/s (Level 3), orbital radius (S_r) 1.5 mm (Level 3), machining time (t_m) 1.401 s (Level 3) and flushing time (t_f) 0.067 s (Level 1). Table 4 shows the results of analysis of variance for MRR. It is observed that all parameters are statistically significant however, peak current (I_p) is most contributing parameter followed by flushing time (t_f) and orbital speed (S_o) in determining the MRR.

From Fig. 5a, it can be observed that MRR increases with increase in peak current. Higher peak current leads to higher discharge energy between the electrodes. Higher discharge energy increases the removal of material per unit time. Similar observation has been reported by Sundaram et al. [19] and Kuppan et al. [20]. Plot of peak current (I_p) in Fig. 5a, reveals that the change in average response between lower and middle value (6 and 13A) is more than that of between middle and higher level of peak current (13 and 21A). It means increment in peak current from 6 to 13A has resulted higher MRR than that of from 13 to 21A peak current. At higher amperage of peak current, possibility of arcing increases in the working gap because higher peak current removes the material at higher rate. These eroded materials (large volume) accumulate and decrease the gap between tool electrode and work surface resulting
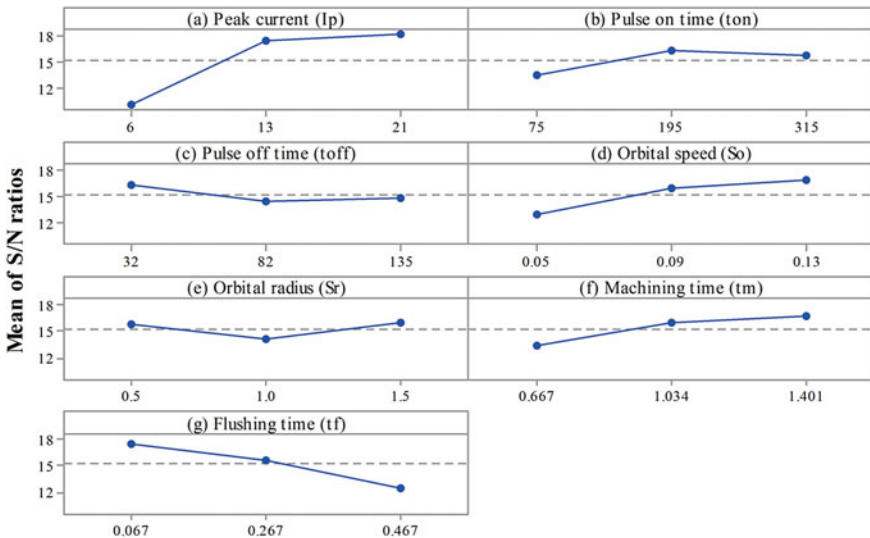

Fig. 5 Main effect plots for MRR

Table 4 ANOVA of S/N ratio for MRR

Source	DF	Sum of square	Mean square	F-Value	P-Value	% Contribution
A: Peak current (I_p)	2	364.033	182.016	322.71	0.00	52.26
B: Pulse on time (t_{on})	2	39.783	19.891	35.27	0.00	5.71
C: Pulse off time (t_{off})	2	17.657	8.828	15.65	0.00	2.53
D: Orbital speed (S_o)	2	74.711	37.355	66.23	0.00	10.73
E: Orbital radius (S_r)	2	17.299	8.649	15.33	0.00	2.48
F: Machining time (t_m)	2	56.031	28.015	49.67	0.00	8.04
G: Flushing time (t_f)	2	120.318	60.159	106.66	0.00	17.27
Error	12	6.768	0.564			0.97
Total	26	696.6				

into arcing. In case of radial orbital EDM, tool electrode retracts back to avoid such arcing and the repetitive retraction of tool electrode adds extra time to the total machining time. Therefore, increment in MRR at higher level of peak current is smaller than that of lower peak current. Further, Analysis of Variance (ANOVA) is performed to obtain the percentage contribution and significance of factors. The calculations for variance (ANOVA) are performed following the procedure explained by Montgomery and Runger [21] and the same is verified with the help of trial version statistical software MINITAB. ANOVA for MRR is shown in Table 4. Table 4 infers that peak current (I_p) represents a major portion of total variation of the observed result. It contributes 52.26% in order to control the total variability. Since its P value is <0.05 (95% confidence interval) therefore peak current (I_p) is statically significant in analyzing MRR.

The effect of Pulse on time (t_{on}) on MRR is illustrated in Fig. 5b. MRR first increases then marginally decreases in radial orbital EDM process. At the middle level of t_{on} (195 μs) the highest MRR is observed. These results are in agreement with the researchers Sohani et al. [22] in die-sinking EDM process. The reason behind such observation may be attributed to the available energy during pulse duration. When pulse on time is short then the energy produced at the point of spark is less which in turn removes lesser material. The spark energy increases with the increase in pulse duration which removes relatively larger material from the workpiece. However, extra long pulse on time distributes the heat energy over larger area through conduction, due to which lesser material is removed from the workpiece. Further, form ANOVA shown in Table 4, it can be observed that its percentage contribution is relatively smaller (5.71%), implying that MRR does not vary substantially on varying pulse on time in selected range.

Effect of pulse off time (t_{off}) on MRR in radial orbital EDM is shown in Fig. 5c. It can be observed that MRR decreases with increase in pulse off time (t_{off}). Lower value of pulse off time offers higher MRR. Higher pulse off time (t_{off}) causes longer machining time for removal of same material and hence it decreases the MRR. Similar findings are reported by researchers [23, 24]. The percentage contribution of pulse off time (t_{off}) indicates that it has very low contribution (2.53%) in affecting the MRR in radial orbital EDM process.

As discussed earlier, radial orbital EDM machining involves to and fro movement of tool electrode during the process therefore it is expected to have some effect of orbital parameters on MRR. Effect of orbital speed (S_o) on MRR is plotted in Fig. 5d. MRR is observed increasing with increase in speed of tool electrode (mm/s) during machining. An increase of about 30% in MRR (mm3/min) is observed at highest orbital speed (0.13 mm/s) relative to lower speed of tool electrode during the process. The increasing trend of MRR is due to the increase in speed of tool electrode during radial orbit EDM machining. With increase in speed of tool movement, time consumed in travelling of tool from centre to the machining area decreases and reduces the total machining time that has improved the material removal rate.

Effect of orbital radius (S_r) on MRR is depicted in Fig. 5e. With increase in orbital radius from 0.5 to 1.0 mm MRR is found reducing and during further increment in orbital radius from 1.0 to 1.5 mm MRR increased marginally. This may be a notable observation in radial orbital EDM process, because it allows to generate larger size of hole with using smaller size of tool electrode without sacrificing material removal rate. However, orbital radius (S_r) is found least contributing factor. The same can be observed from the main effect plot in Fig. 5e as its average S/N ratios do not vary much from the mean line.

Plot of machining time in Fig. 5f depicts the variation in MRR with machining time (t_m) in radial orbital EDM process. The mean S/N ratios calculated for MRR is increasing with increase in machining time (t_m). As machining time increases from lower to higher values, an increment about 25% in MRR is observed. Increment in MRR with machining time is due to longer forward step of tool electrode in radial orbital EDM process. As illustrated in Fig. 3, the movement of tool electrode in radial orbital machining is to and fro nature. The length of forward step travelled by tool electrode is decided by machining time in seconds. Larger setting of machining time implies longer step of tool travel during process. Therefore, higher machining time (t_m) reduces the time consumed during tool travelling and hence MRR is improved. The backward movement of tool electrode is controlled by flushing time. Higher the flushing time, longer will be the backward step. Longer flushing time (t_f) duration increases the tool retraction time that is non-cutting time (non productive time). Therefore, MRR is found reducing with increase in flushing time (t_f). The same can be observed from Fig. 5g. However, the percentage contribution of flushing time (t_f) is higher than that of machining time (t_m).

3.2 Analysis of Tool Wear Rate (TWR)

Tool wear is mostly observed on cylindrical surface of tool electrode during radial orbital EDM process. TWR is calculated using Eq. (3). The calculated TWR for each experiment is converted into the S/N ratio. Since TWR is lower the better quality characteristic, hence S/N ratio is calculated using Eq. (4) and shown in Table 3.

Figure 6 shows the main effect plots for TWR. The optimal combination of factors for lower TWR are 6A (Level 1) of peak current (I_p), 315 µs (Level 3) of pulse on time (t_{on}), 32 µs (Level 1) of pulse off time (t_{off}), 0.05 mm/s (Level 1) of orbital speed (S_o), 1.0 mm (Level 2) of orbital radius (S_r), 0.667 s (Level 1) of machining time (t_m) and 0.467 s (Level 3) of flushing time (t_f). Table 5 represents the results of analysis of variance of TWR. It shows that peak current (I_p) and pulse on time (t_{on}) are statistically significant parameters and have major effect over TWR as they collectively share approximately 81% of total sum of square. However, orbital speed (S_o) has relatively less contribution (8.73%) but is statistically significant. Remaining parameters viz., pulse off time (t_{off}), orbital radius (S_r), machining time (t_m) and flushing time (t_f) are observed as insignificant for TWR.

From Fig. 6a, it can be observed that the mean S/N ratio for TWR is maximum at 6A peak current (I_p) and decreases with increase in peak current. This implies that TWR is less at lower current setting. The obtained results are in good agreement with results reported by Lee and Li [24] Heat energy generated between workpiece and tool electrode interface increases with increase in peak current (I_p) that leads to the melting and vaporization of tool material resulting into higher TWR. Wear on tool surface can be clearly observed in the form of craters, as shown in Fig. 7. The size
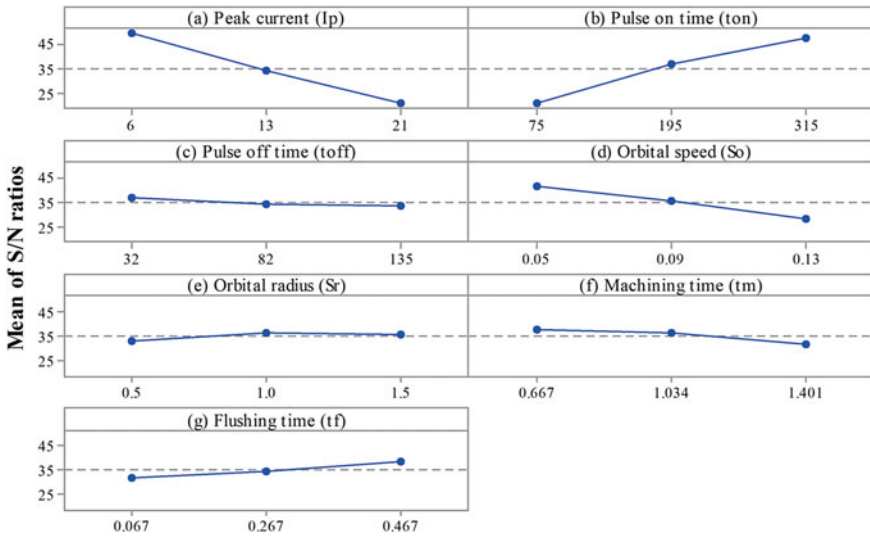

Fig. 6 Main effect plots for TWR

Table 5 ANOVA of S/N ratio for TWR

Source	DF	Sum of square	Mean square	F-Value	P-Value	% Contribution
A: Peak current (I_p)	2	3658.87	1829.43	54.72	0.000	42.80
B: Pulse on time (t_{on})	2	3289.42	1644.71	49.20	0.000	38.48
C: Pulse off time (t_{off})	2	60.87	30.43	0.91	0.428	0.71
D: Orbital speed (S_o)	2	745.81	372.91	11.15	0.002	8.73
E: Orbital radius (S_r)	2	66.39	33.19	0.99	0.399	0.78
F: Machining time (t_m)	2	147.8	73.9	2.21	0.152	1.73
G: Flushing time (t_f)	2	177.53	88.76	2.66	0.111	2.08
Error	12	401.18	33.43			4.69
Total	26	8547.86				

of these micro craters increases with increase in peak current. From ANOVA shown in Table 5, peak current (I_p) is the highest contributing (42.8%) factor amongst all selected factors.

Figure 6b shows the relationship between TWR and pulse on time (t_{on}) during boring operation in radial orbital EDM process. It can be seen that S/N ratio of TWR is higher at higher pulse on time (315 µs) and lower at lower pulse on time (75 µs) which implies that TWR decreases with the increase in pulse on time (t_{on}). Similar results are reported by Zarepour et al. [25] and Barenji et al. [26]. Increment in pulse on time (t_{on}) decreases the spatial current density and also increases the carbon deposition on tool surface that protects the tool electrode from wear [22]. Analysis of variance shown in Table 5 indicates that pulse on time (t_{on}) is statistically significant factor (P value < 0.05) and its percentage contribution is 38.48%.

The relationship between pulse off time (t_{off}) and mean S/N ratios of TWR is shown in Fig. 6c. As evident from Table 5, pulse off time (t_{off}) has insignificant effect on TWR; it shares only 0.71% contribution in controlling the variance of TWR. Figure 6c reveals that there is marginal change in S/N ratio of TWR on changing pulse off time (t_{off}) from lower to higher setting values. However, at lower pulse off time (t_{off}), minimum TWR is obtained.

The effect of orbital speed (S_o) on TWR is depicted in Fig. 6d. Change in orbital speed (S_o) has significantly affected the TWR during radial orbital EDM process. The mean S/N ratio for TWR has reduced to approx. 31% on changing orbital speed (S_o) from lower to higher (0.05 and 0.13mm/s) setting. Least TWR is observed at lowest orbital speed. The reason for higher TWR at higher orbital speed of tool electrode is the frequent sparking. Increment in orbital speed reduces the tool travelling time inside the cavity during radial orbital machining. This means tool electrode
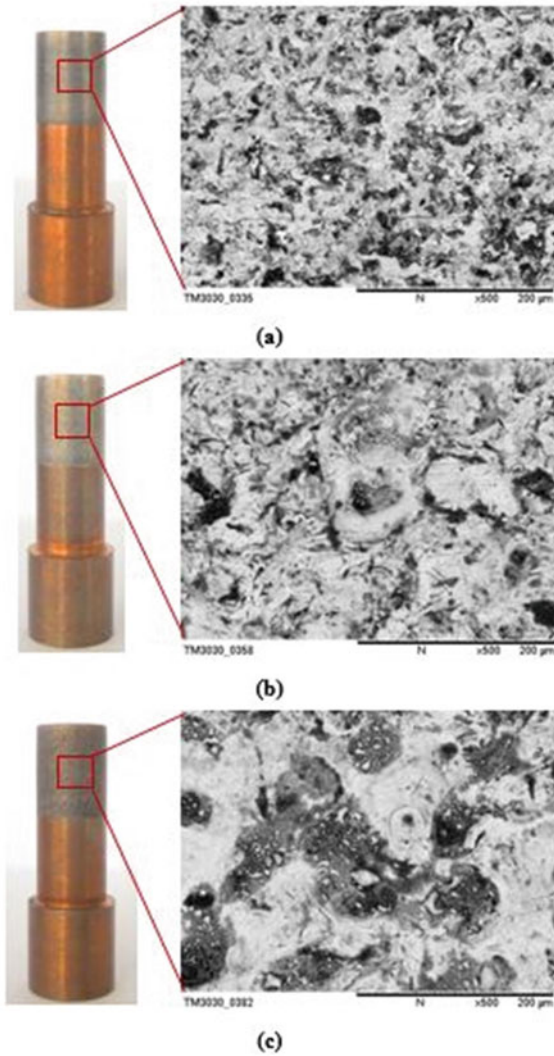
Fig. 7 Micrograph of tool surface at **a** $I_p = 6$A, $t_{on} = 75$ µs, **b** $I_p = 13$A, $t_{on} = 75$ µs, **c** $I_p = 21$A, t_{on} 75 µs

will complete the to and fro movement on radial distance quickly and tool electrode remains in contact with spark frequently that reduces the cooling as well as conduction time in turn increasing the erosion rate of tool electrode. On other hand, at lower orbital speed, tool electrode provides sufficient time for cooling and conducting heat that resulting into lower TWR in radial orbital EDM process. Analysis of variance for TWR shown in Table 5 indicates that orbital speed (S_o) has only 8.73% of contribution amongst others selected factors.

Effect of remaining factors such as orbital radius (S_r), machining time (t_m) and flushing time (t_f) has minimal effect on TWR as shown in Fig. 6e–g respectively. The insignificance of these factors can also be observed from Table 5; these factors collectively contribute about 4.5% in reducing the variance of TWR. However, maximum TWR is observed at lowest orbital radius (0.5 mm) and further increment in orbital radius from 1.0 to 1.5 mm caused little change in S/N ratios of TWR. It is worth noting that TWR is not significantly affected by orbital radius (S_r) and therefore any size of tool electrode can be used to enlarge cavity.

The effect of flushing time (t_f) for TWR in radial orbital EDM process is illustrated in Fig. 6g. The result shows that in radial orbital EDM, TWR is decreasing with increase in flushing time (t_f). Higher flushing time has resulted into minimum TWR. Flushing time implies the time duration of tool retracting during radial orbital EDM process. Higher the flushing time, larger will be the retracting distance of tool electrode from the machining zone. Higher flushing time provides sufficient time to tool electrode during radial orbital machining due to which TWR is observed decreasing with flushing time.

TWR does not conclude the nature of tool wear, it only gives the quantitative idea of wear. Therefore, in order to observe the wear on tool electrode, the cylindrical surface as well as bottom surface is considered for the investigation. Figures 7 and 8 show the side wear on cylindrical and bottom surfaces respectively of tool electrode used for boring operation at different peak current. It is observed that wear is mainly concentrated on cylindrical surfaces than that of bottom surfaces. This is due to the nature of tool movement during radial orbital machining process. As illustrated in Fig. 2b the tool electrode moves only in lateral direction and therefore major portion of cutting of material during this process takes place only through the cylindrical surface of tool electrode. Relatively lesser wear is observed on bottom surface of tool electrode is observed, this is because the tool electrode. Figure 8 shows the bottom end of tool electrode (taken at × 35 magnification using VMS) used for boring operation at different peak currents using radial tool movement in EDM process. Wear on bottom surface of tool electrode can be observed in the form of
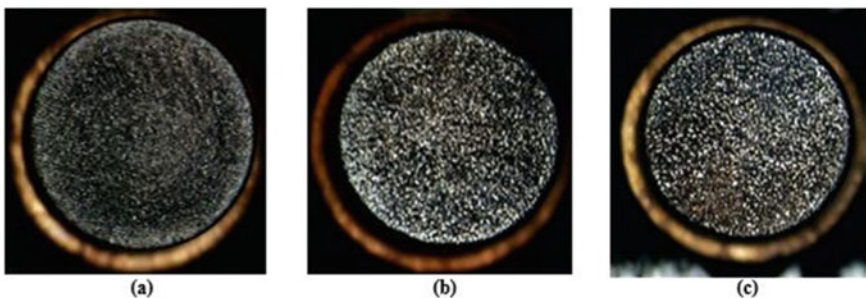

Fig. 8 Image of bottom surface of tool electrode at **a** $I_p = 6$A, $t_{on} = 75\,\mu$s **b** $I_p = 13$A, $t_{on} = 75\,\mu$s **c** $I_p = 21$A, $t_{on} = 75\,\mu$s
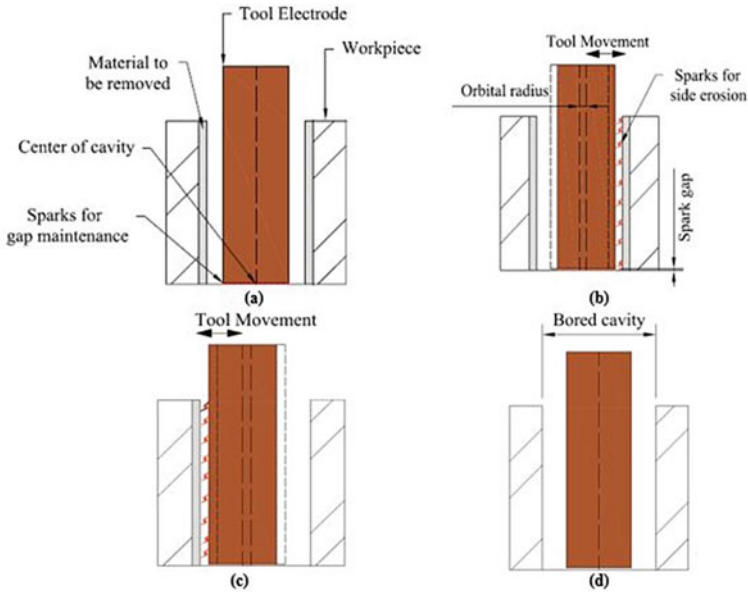
Fig. 9 Sparking phenomenon during radial EDM process. **a** Start of the process. **b** Removal of material in positive X direction. **c** Removal of material in negative X direction. **d** End of process

tiny crates which occurs due to few sparks that occur between bottom surfaces of tool electrode and cavity to maintain the spark gap.

From schematic representations of boring operation shown in Fig. 9, it can be observed that size of the cavity is being increased with sparks generated at side surface of tool electrode and the bottom end of tool electrode is engaged only for spark gap maintenance. Thus it can be understood that major portion of material is worn out from the cylindrical side surface of the tool electrode unlike the usual die sinking EDM process where tool wear occurs mainly on the bottom end surface.

3.3 Analysis of Surface Roughness (Ra)

As discussed in Sect. 3.2, the size of the cavity is enlarged mainly by cutting the materials from side walls of cavity and removal of materials from the bottom end of cavity is negligible during radial tool movement in EDM process. Therefore, in the present work surface roughness is measured on the side surface of cavity that is generated by radial movement of the tool electrode.

Main effect plots of Ra are plotted using mean of S/N ratios at each level for each factor and shown in Fig. 10. Analysis of S/N ratio reveals that the optimal parametric combination for lower surface roughness value (Ra) during radial orbital
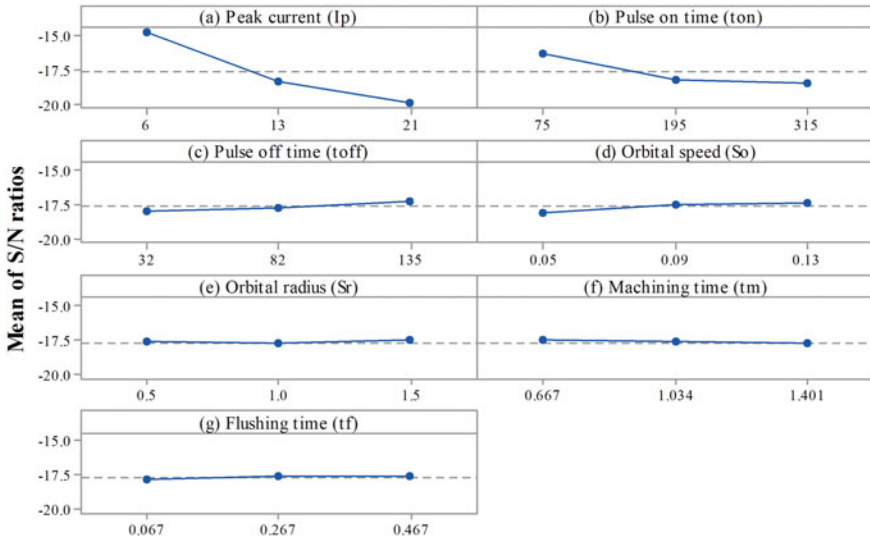
Fig. 10 Main effect plots for Ra

EDM process is 6A (Level 1) peak current (I_p), 75 μs (Level 1) pulse on time (t_{on}), 135 μs (Level 3) pulse off time (t_{off}), 0.13 mm/s (Level 3) orbital speed (S_o), 1.5 mm (Level 3) orbital radius (S_r), 0.667 s (Level 1) machining time (t_m) and 0.467 s (Level 3) flushing time (t_f). Table 6 contains the results of ANOVA for surface roughness.

Table 6 ANOVA of S/N ratio for Ra

Source	DF	Sum of square	Mean square	F-Value	P-Value	% Contribution
A: Peak current (I_p)	2	126.717	63.3585	383.023	0.000	80.21
B: Pulse on time (t_{on})	2	23.748	11.874	71.782	0.000	15.03
C: Pulse off time (t_{off})	2	2.475	1.2375	7.481	0.008	1.57
D: Orbital speed (S_o)	2	2.089	1.0445	6.314	0.013	1.32
E: Orbital radius (S_r)	2	0.293	0.1465	0.885	0.427	0.19
F: Machining time (t_m)	2	0.187	0.0935	0.565	0.583	0.12
G: Flushing time (t_f)	2	0.493	0.2465	1.490	0.264	0.31
Error	12	1.985	0.165417			1.26
Total	26	157.987				

Peak current (I_p) and pulse on time (t_{on}) are the major contributing parameters followed by pulse off time (t_{off}). Peak current (I_p), pulse on time (t_{on}), pulse off time (t_{off}) and orbital speed (S_o) are statistically significant parameters whereas orbital radius (S_r), machining time (t_m) and flushing time (t_f) are statistically insignificant parameters.

Figure 10a shows the effect of peak current (I_p) on surface roughness value (Ra). It can be observed that mean value of S/N ratio for Ra decreases with increase in peak current. It implies that surface roughness value (Ra) increases with increase in peak current. The obtained results are in good agreement with the results reported by Gostimirovic et al. [27]. Increase in peak current (I_p) increases the discharge energy between the tool electrode and the workpiece in EDM process. Removal of material takes place from workpiece at the end of spark leaving behind tiny craters in EDM process. The size of crater depends upon the discharge energy. Typical images of workpiece surfaces are shown in Fig. 11a–b. At lower peak current i.e. at 6A, the crater sizes are relatively smaller than that observed at highest peak current of 21A. High peak current has generated deeper and more irregular craters that have resulted higher surface roughness. The percentage contribution calculated in Table 6 represents the relative power of peak current (I_p) (80.21%) to reduce the variation.

The effect of pulse on time (t_{on}) on Ra value is shown in Fig. 10b. The S/N ratio of average surface roughness value (Ra) at lower pulse on time (t_{on}) is higher and is found minimum at longer pulse on time (t_{on}). This means lower pulse on time has resulted smother surface than higher pulse on time. From Fig. 12a–b it can be clearly observed that the size of craters are smaller as well as outer rings of these craters are relatively thin than that of craters generated at higher pulse on
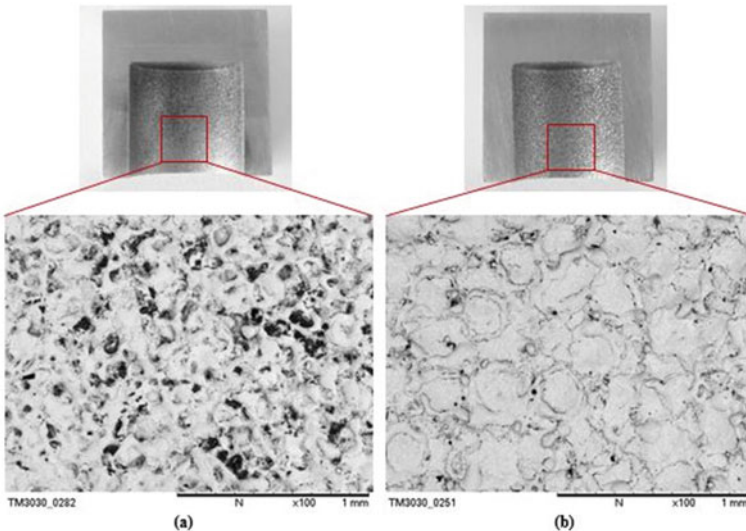

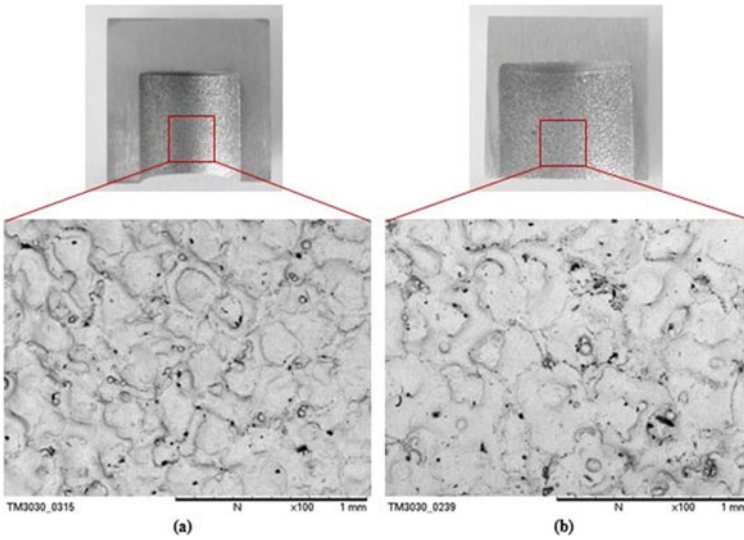**Fig. 11** Micrographs of machined surface generated at **a** lowest I_p = 6A **b** highest I_p = 21A

Fig. 12 Micrographs of machined surface generated at **a** lowest $t_{on} = 75\,\mu s$ **b** highest $t_{on} = 315\,\mu s$

time. Similar results are reported by Kiyak and Cakır [28]. Pulse on time (t_{on}) is the second most significant factor, as shown in Table 6; it shares 15.03% of contribution in controlling the variance of surface roughness value (Ra) during boring operation with radial orbital EDM process.

The effect of remaining parameters like, pulse off time (t_{off}), orbital speed (S_o), orbital radius (S_r), machining time (t_m) and flushing time (t_f) are marginal. This can be clearly observed from Fig. 10c–f, as the variation in S/N ratios between lower level and higher level are minimum or negligible. Their effect on surface roughness value (Ra) can also be statistically quantified using ANOVA shown in Table 6, their collectively percentage of contribution is only 3.5%.

4 Confirmation Tests

Confirmation experiments are important to verify the results as well as to confirm the reproducibility of experiments. A confirmation experiment is performed by conducting a test using a specific combination of the factors and levels previously evaluated. The following steps are involved in conducting a confirmation experiments:

1. Determination of the preferred combination of the levels of the process parameters by the analysis.
2. Calculation of estimated mean for preferred combination of the levels.
3. Calculation of the confidence interval value.

Table 7 Confirmation test results

Responses	Optimum level	Predicted S/N ratio (η_P) (db)	Experimental S/N ratio (η_E) (db)	% Prediction error $\left\|\frac{\eta_E - \eta_P}{\eta_E} \times 100\right\|$
MRR	$A_3B_2C_1D_3E_3F_3G_1$	26.4416	26.2728	0.64
TWR	$A_1B_3C_1D_1E_2F_1G_3$	68.3879	64.2931	6.36
R_a	$A_1B_1C_3D_3E_3F_1G_3$	−12.7964	−13.3037	3.81

4. Calculation of the confidence interval for the true mean around estimated mean.
5. Conduction of tests under preferred combination of process parameters.
6. Comparison of the confirmation test average result to the confidence interval for true mean.

Taguchi recommends the prediction of responses at optimum setting of parameters [29]. Optimum combination of process parameters as stated in step 1 has been obtained by the analysis of MRR, TWR and surface roughness in Sects. 3.1, 3.2 and 3.3 respectively.

4.1 Estimation of Predicted Means

The estimated mean of MRR, TWR and Ra are calculated using following Eq. (5) [17].

$$\eta_P = T + \sum (\eta_i - T) \tag{5}$$

where, T is overall mean of response parameter, η is average value of significant parameters.

The confirmation tests are performed on the optimal setting of parameters. The S/N ratios of obtained at the optimum combination of parameters and the predicted results are shown in Table 7. This shows that the optimum factors level combination for these experiments are very close to the predicted S/N ratio.

5 Conclusions

This study employs radial tool movement in EDM process for boring operation on Inconel 718 material. Experiments are performed using Taguchi method and the observed results are analysed using ANOVA. Following important conclusions can be drawn from this study:

1. Boring of predrilled cavity can be successfully achieved in EDM process using radial tool movement.
2. Boring operation in EDM process is not affected by bore size because tool wear rate and surface roughness is not significantly affected by orbital radius.
3. Peak current is found to be the most influencing parameter in boring operation in edm process.
4. Speed of the tool electrode during boring operation significantly affects the material removal rate, tool wear rate and surface roughness. With increase in speed, MRR increases but TWR and surface roughness (Ra) decreases.
5. Surface quality and tool wear rate does not depend on to and fro movement of tool electrode on radial path because machining time and flushing time has negligible effect on responses.

This study introduces the possibility of boring operation in electro discharge machining process. Several factors involved during machining have been analyzed, however in future one can study the dimensional accuracy of bored cavity that can be achieved in radial orbital EDM process.

References

1. Jahan MP, Rahman M, Wong YS (2011) A review on the conventional and micro-electrodischarge machining of tungsten carbide. Int J Mach Tools Manuf 51:837–858
2. Yadav US, Yadava V (2015) Experimental modeling and multiobjective optimization of electrical discharge drilling of aerospace superalloy material. Proc IMechE, Part B: J Eng Manuf 229:1764–1780
3. Lascoe OD (1988) Handbook of fabrication processes. ASM Int, Metal Park, Ohio
4. Dave HK, Desai KP, Raval HK (2013) A Taguchi approach-based study on effect of process parameters in electro discharge machining using orbital tool movement. Int J Mach Mach Mater 13:52–66
5. El-Taweel T, Hewidy M (2009) Enhancing the performance of electrical-discharge machining via various planetary modes. Int J Mach Mach Mater 5:308–320
6. Bamberg E, Heamawatanachai S (2009) Orbital electrode actuation to improve efficiency of drilling micro-holes by micro-EDM. J Mater Process Technol 209:1826–1834
7. Jain VK (2012) Advance machining processes. Allied Publishers Pvt, Ltd., New Delhi
8. Belgassim O, Abusaada A (2011) Investigation of the influence of EDM parameters on the overcut for AISI D3 tool steel Proc IMechE, Part B: J Eng Manuf. https://doi.org/10.1177/0954405411400498
9. Singh A, Kumar P, Singh I (2013) Electric discharge drilling of metal matrix composites with different tool geometries. Proc IMechE, Part B: J En Manuf 227:1245–1249
10. Jabbaripour B, Sadeghi M, Faridvand S, Shabgard M (2012) Investigating the effects of EDM parameters on surface integrity, MRR and TWR in machining of Ti–6Al–4V. Mach Sci Technol 16:419–444
11. Muthuramalingam T, Mohan B (2013) Influence of discharge current pulse on machinability in electrical discharge machining. Mater Manuf Process 28:375–380
12. Sivam SP, Michaelraj AL, Kumar SS, Prabhakaran G, Dinakaran D, Ilankumaran V (2014) Statistical multi-objective optimization of electrical discharge machining parameters XE "Machining parameters" in machining titanium grade 5 alloy using graphite electrode. Proc IMechE, Part B: J Eng Manuf 228:736–743

13. Kolli M, Kumar A (2015) Effect of dielectric fluid with surfactant and graphite powder on Electrical Discharge Machining of titanium alloy using Taguchi method. Eng Sci Technol, Int J 18:524–535
14. Rajurkar K, Royo G (1989) Effect of RF control and orbital motion on surface integrity of EDM components. J Mech Work Technol 20:341–352
15. Yu ZY, Rajurkar KP, Shen H (2002) High aspect ratio and complex shaped blind micro holes by micro EDM. CIRP Ann Manuf Technol 51:359–362
16. Bamberg E, Heamawatanachai S, Jorgensen JD (2005) Flexural micro-EDM head for increased productivity of micro-holes. ASPE Conf Norfolk 82–85
17. Ross PJ (2005) Taguchi techniques for quality engineering: loss function, orthogonal experiments, parameter and tolerance design. McGraw Hill Education, New Delhi
18. Phadke MS (1995) Quality engineering using robust design. Prentice Hall PTR, New Jersey
19. Sundaram MM, Pavalarajan GB, Rajurkar KP (2008) A study on process parameters of ultrasonic assisted micro EDM based on Taguchi method. J Mater Eng Perform 17:210–215
20. Kuppan P, Rajadurai A, Narayanan S (2008) Influence of EDM process parameters in deep hole drilling of Inconel 718. Int J Adv Manuf Technol 38:74–84
21. Montgomery DC, Runger GC (2010) Applied statistics and probability for engineers. Wiley, New York
22. Sohani MS, Gaitonde VN, Siddeswarappa B, Deshpande AS (2009) Investigations into the effect of tool shapes with size factor consideration in sink electrical discharge machining (EDM) process. Int J Adv Manuf Technol 45:1131–1145
23. Eyercioglu O, Cakir MV and Kursad G (2013) Influence of machining parameters on the surface integrity in small-hole electrical discharge machining. Proc IMechE, Part B: J Eng Manuf. https://doi.org/10.1177/0954405413498730
24. Lee S, Li X (2001) Study of the effect of machining parameters on the machining characteristics in electrical discharge machining of tungsten carbide. J Mater Process Technol 115:344–358
25. Zarepour H, Tehrani AF, Karimi D, Amini S (2007) Statistical analysis on electrode wear in EDM of tool steel DIN 1.2714 used in forging dies. J Mater Process Technol 187:711–714
26. Barenji RV, Pourasl HH, Khojastehnezhad VM (2016) Electrical discharge machining of the AISI D6 tool steel: prediction and modeling of the material removal rate and tool wear ratio. Precis Eng 45:435–444
27. Gostimirovic M, Kovac P, Sekulic M, Skoric B (2012) Influence of discharge energy on machining characteristics in EDM. J Mech Sci Technol 26:173–179
28. Kiyak M, Cakır O (2007) Examination of machining parameters on surface roughness in EDM of tool steel. J Mater Process Technol 191:141–144
29. Taguchi G, Chowdhury S, Wu Y (2005) Taguchi's quality engineering handbook. Wiley, New Jersey